Biochimica et Biophysica Acta, 974 (1989) 54–65
Elsevier

BBA 42953

Heterogeneity of the $P^+Q_A^-$ recombination kinetics in reaction centers from *Rhodopseudomonas viridis*: the effects of pH and temperature

Pierre Sebban [1] and Colin A. Wraight [2]

[1] *Laboratoire de Photosynthèse du CNRS, ER 307, Bât. 24, CNRS Gif-sur-Yvette (France) and* [2] *Department of Physiology and Biophysics and Department of Plant Biology, University of Illinois, Urbana, IL (U.S.A.)*

(Received 5 July 1988)
(Revised manuscript received 21 November 1988)

Key words: Bacterial photosynthesis; Reaction center; Charge recombination; pH dependence; Protonation; (*Rps. viridis*)

The decay of the flash-induced absorbance changes related to the primary electron donor, P^+, was measured in reaction centers from *Rhodopseudomonas viridis*. The decay, which occurs by the recombination or back-reaction of $P^+Q_A^-$, was found to be not a single exponential and could be decomposed into two components. At pH 9, in the presence of *o*-phenanthroline, the two phases exhibited rate constants of 350 ± 25 s^{-1} (k_{slow}) and 1400 ± 100 s^{-1} (k_{fast}). In the absence of *o*-phenanthroline, in Q_B-depleted reaction centers, the rate constants were 370 ± 25 and 1700 ± 100 s^{-1}, respectively. k_{slow} and k_{fast} display temperature-dependences similar to those previously described by Shopes and Wraight ((1987) Biochim. Biophys. Acta 893, 409–425) for the total decay component. Down to 240 K, the temperature-dependences of k_{slow} and k_{fast} indicate thermally activated processes, which are presumed to proceed by repopulation of the P^+I^- state from $P^+Q_A^-$. At temperatures below 240 K, an activationless process dominates with rate constants for the two phases which depend somewhat on the concentration of glycerol. In aqueous buffer, the limiting values at low temperatures, k_{Tslow} and k_{Tfast}, were determined to be 155 ± 10 and 460 ± 60 s^{-1}, respectively. After correction for these limiting rates, the ambient temperature-dependences were linear in an Arrhenius plot. At pH 9, the activation energies (enthalpies, ΔH) were 0.258 ± 0.009 and 0.278 ± 0.021 eV for the slow and fast phases, respectively. The entropies of activation were also quite large. Consequently the activation free energies (ΔG) were inverted compared to the activation enthalpies, i.e., $\Delta G_{slow} = 0.292 \pm 0.011$ eV and $\Delta G_{fast} = 0.260 \pm 0.022$ eV. k_{slow} and k_{fast} were also significantly pH-dependent. As the pH was raised from pH 6, both rate constants showed a shallow minimum at pH 7.5–8, and accelerated significantly as the pH was raised further. The pH-dependence of both components was more marked in the absence than in the presence of *o*-phenanthroline. The relative proportions of k_{slow} and k_{fast} were also strongly pH-dependent in the range pH 5.5–11.5. The amplitude curves displayed two waves that were dependent on ionic conditions and on the presence of *o*-phenanthroline. The pH- and temperature-dependences of the rates and amplitudes of the recombination components are interpreted in terms of multiple protonation states of the reaction center affecting the energetics of the thermally activated recombination pathway. The pH-dependence of the rates can be understood as arising from the electrostatic stabilization of the charge-separation states, $P^+Q_A^-$ and P^+I^-, due to the interaction of at least two protonation sites with the species Q_A^- and I^-. The pH-dependence of the recombination rates, in the range pH 5.5–10, could be accounted for in this way, with two distinct values for pK_{Q_A}: one with pK_{Q_A} about 6, for which protonation resulted in the relative stabilization of P^+I^-, decreasing ΔG and leading to acceleration of the back-reaction, and one with pK_{Q_A} about 9, which relatively stabilized $P^+Q_A^-$ in the protonated state, increasing ΔG and causing slower recombination. The biphasicity of the recombination kinetics in this pH range was ascribed to the comparable rates of the back-reaction and of protonation of the reaction center at most pH values. Thus, the distribution of protonation states established in the dark cannot fully reequilibrate with the new pK values of the

Abbreviations: CAPS, cyclohexylaminopropane sulfonic acid; Mes, 4-morpholineethanesulfonic acid; RC, reaction center; LDAO, lauryl dimethylamine-*N*-oxide.

Correspondence: C.A. Wraight, Department of Physiology and Biophysics and Department of Plant Biology, University of Illinois, 505 S. Goodwin Ave., Urbana, IL 61801, U.S.A.

charge-separated state, on the timescale of the back-reaction. The behavior described here for the $P^+Q_A^-$ charge recombination in *Rps. viridis* is in contrast to that in *Rhodobacter sphaeroides*, which exhibits monophasic back reaction kinetics at ambient temperatures. It is suggested that in the latter species the back-reaction is sufficiently slow ($k = 10\ s^{-1}$) that protonation states present after the flash can equilibrate prior to the charge recombination.

Introduction

Light energy absorbed by, or transferred to, reaction centers of photosynthetic organisms drives a charge separation with a yield close to 1. The structure of the reaction center (RC) from purple bacteria is now becoming well known, due to the successful crystallization and X-ray structural analysis of RCs from *Rps. viridis* [1,2] and *Rb. sphaeroides* [3–6]. This work, and sequence comparisons with other bacteria and with Photosystem II of plants, suggests a substantially conserved structure between diverse species [7,8]. The bacterial RC's are protein complexes, consisting of three polypeptides of similar molecular mass (30–35 kDa), named L, M and H. The L and M polypeptides show distinct homology and, as a heterodimer, carry all the pigments and cofactors involved in the photochemical charge separation. This is accomplished between the primary donor, P, a dimer of bacteriochlorophyll (Bchl), and a molecule of quinone, Q_A. A bacteriopheophytin (Bph), I, functions as an intermediate in the electron transfer from P to Q_A. In some species, including *Rps. viridis*, there is a fourth polypeptide of the RC complex, the C subunit, containing *c*-type hemes [9].

In *Rb. sphaeroides*, Q_A is ubiquinone and the chlorin pigments are Bchl *a* and Bph *a*; the free energy difference from P* to $P^+Q_A^-$ is 0.86 eV, and from P^+I^- to $P^+Q_A^-$ is about 0.46–0.64 eV, depending on the degree of relaxation of P^+I^- [10,11]. In *Rps. viridis*, Q_A is menaquinone and the pigments are Bchl *b* and Bph *b*; these differences presumably contribute to the fact that the energy spacing between the charge-separation states is significantly smaller in *Rps. viridis* than in *Rb. sphaeroides* [12,13]. When the secondary quinone, Q_B, is absent, or when inhibitors of Q_A to Q_B electron transfer are present, the $P^+Q_A^-$ state recombines in about 100 ms in *Rb. sphaeroides* and about 1 ms in *Rps. viridis*. The temperature-dependences of the $P^+Q_A^-$ recombination kinetics are also very different in these two species. In *Rb. sphaeroides* the rate constant of charge recombination increases slightly as the temperature decreases to 80 K, whereas in *Rps. viridis* it decreases, according to a thermally activated process, as the temperature decreases to about 250 K, whereafter the rate constant is temperature-independent down to 80 K [13]. Similar behavior is observed for the recombination kinetics of *Rb. sphaeroides* RCs in which the native Q_A has been replaced by low-potential analogs [13–16]. These results led to the suggestion that, in such cases, the $P^+Q_A^-$ recombination occurs by two competitive pathways: a direct electron-tunneling process that dominates at low (under 250 K) temperatures and a thermally activated process that is predominant at room temperature [13–16]. The latter route proceeds via an energetically elevated intermediate state that has been identified with P^+I^-, or some closely related entity. The availability of this path, which is species-dependent and experimentally manipulable through the potential of the Q_A/Q_A^- redox couple, is determined by the free energy difference between $P^+Q_A^-$ and P^+I^-.

The rate of recombination of the $P^+Q_A^-$ state in *Rps. viridis* was also found to be pH-dependent, becoming faster as the pH was raised above 9 and levelling off above pH 10.5 [13]. This behavior was interpreted in terms of protonation of a site that lies between I and Q_A with pK values of 9.4 and 9.7 in the states, I^-Q_A or IQ_A^-, respectively, thereby causing differential stabilization of the two charge-separation states, P^+I^- and $P^+Q_A^-$, and modifying the energy difference between them.

In this paper, we describe heterogeneity in the $P^+Q_A^-$ recombination kinetics of *Rps. viridis*. We interpret our results in terms of multiple protonation states of the reaction center, together with the fact that the recombination kinetics in *Rps. viridis* are sufficiently fast (in contrast to the slower kinetics in *Rb. sphaeroides*) to prevent the different states of protonation of $P^+Q_A^-$ from equilibrating, prior to the return to the ground state PQ_A.

Materials and Methods

Reaction centers from *Rps. viridis* were prepared as described previously [17], except that the elution from the DEAE-cellulose column was done in 120 mM NaCl. The residual Q_B content was in the range 5–10%. When needed, Q_B was further removed by the method of Okamura et al. [18]. *O*-Phenanthroline was used at a concentration of 4 mM.

The kinetic spectrophotometer apparatuses were as described by Shopes and Wraight [13,17], for both room-temperature and low-temperature measurements. The typical RC concentrations for the kinetic absorption measurements were 0.75 μM at room temperature and 20 μM at low temperature. The bound cytochromes were chemically oxidized by the addition of 1–2 mM ferricyanide to the RC stock, which was then dialysed against 10 mM Tris (pH 8)/100 mM NaCl0.1% LDAO (Ammonyx LO). The ferricyanide concentration in the cuvette was less than 0.1 μM, a precaution necessary at

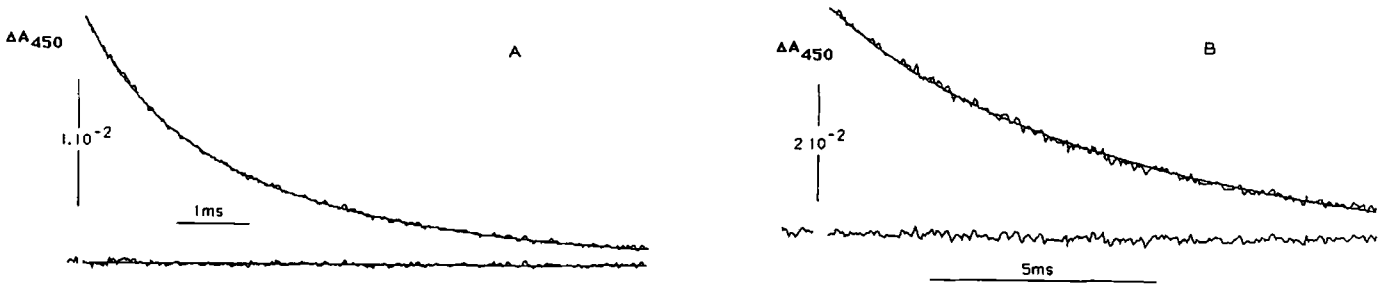

Fig. 1. Charge recombination in *Rps. viridis* RCs, measured at 450 nm. (A) Kinetics at room temperature; the decay was fitted by the sum of two exponentials with lifetimes of 0.77 and 2.85 ms and relative amplitudes of 0.35 and 0.65, respectively. The difference between the experimental and fitted curves is shown below. Conditions: 20 mM Tris-HCl (pH 9)/100 mM NaCl/4 mM *o*-phenanthroline/0.1% LDAO, 20 °C. (B) Kinetics at low temperature; the curve fitting corresponds to two exponentials with lifetimes of 8.8 and 2.4 ms and relative amplitudes of 0.85 and 0.15, respectively. Conditions as for (A), but with 60% glycerol, 110 K.

pH values below 9 to avoid rapid oxidation of Q_A^- by ferricyanide [17]. However, at pH values above 9 this is not a problem and ferricyanide was added, up to 20–60 μM, to maintain the redox potential at about 450 mV, sufficient to keep the cytochromes oxidized.

Exponential analyses of the kinetics were performed by a modified Marquardt algorithm, run on an LSI 11/23 or 11/73 computer (DEC), as described elsewhere [19].

The pH buffers were 20 mM Mes below 7.3, 20 mM Tris-HCl in the range 7.3–9, 10 mM Tris plus 10 mM potassium pyrophosphate in the pH range 9–10 and 20 mM CAPS above 10. The standard error on pH measurements was 0.05 units. Temperature was measured with an iron-constantan thermocouple, with a precision of 0.3 °C.

Results

Heterogeneity of the charge recombination kinetics

The recombination of $P^+Q_A^-$ observed at 450 nm in the presence of *o*-phenanthroline (4 mM), at pH 9 and 20 °C, is shown in Fig. 1. The decay curve was fit by the sum of two exponentials with lifetimes of 2.85 and 0.77 ms, and relative amplitudes of 65 and 35%, respectively. In the following, the rate constant of these two decay phases will be denoted k_{slow} and k_{fast}, and their relative amplitudes, A_{slow} and A_{fast}. The overall rate constant (k_{total}), determined from a one-component analysis, was 490 s^{-1}, in fair agreement with the data of Shopes and Wraight [13], who reported a rate of 560 s^{-1} in 0.1% Triton X-100. The same kinetic decomposition was obtained in the near-infra-red bands of the spectrum at 800, 850 or 960 nm. However, the A_{slow}/A_{fast} ratio changed dramatically near the $PQ_A/P^+Q_A^-$ isosbestic point at 833 nm (Fig. 2). Just below this wavelength, at 832.5 nm, the ratio is at least 0.9, whereas just above, at 834.5 nm, it is not greater than 0.1. The spectral difference between the two components is very slight and was only detectable at wavelengths very close to the isosbestic points for the $P^+Q_A^-$ back-reaction.

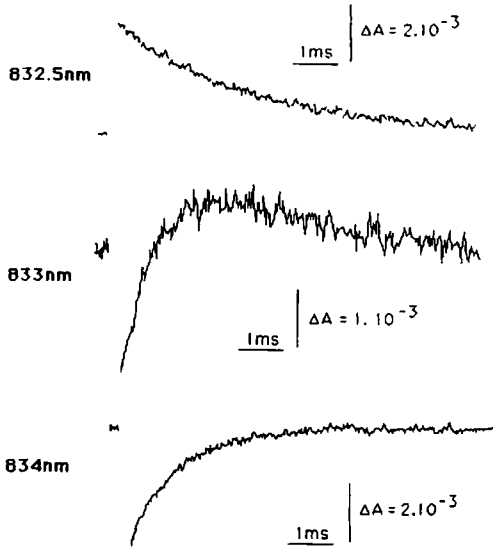

Fig. 2. Room-temperature decay kinetics of the charge recombination in *Rps. viridis* RCs, measured near the isosbestic point. At 832.5 nm (top), the decay is close to monoexponential with a lifetime of 2.8 ms. At 833 nm (middle), two components are present with lifetimes of 2.8 and 0.8 ms, with opposite contributions to the light-induced absorption change. At 834 nm (bottom), the decay curve is again close to monoexponential, but with a lifetime of 0.8 ms. Conditions as in Fig. 1.

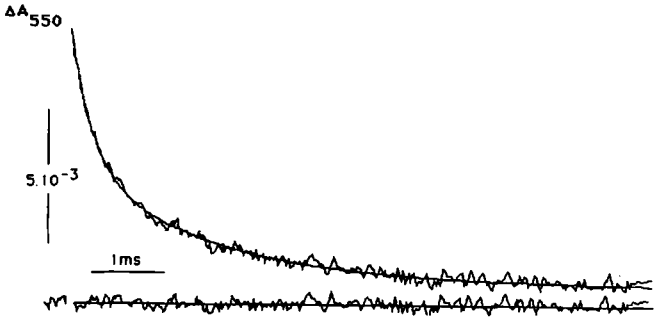

Fig. 3. Charge-recombination kinetics measured in *Rps. viridis* chromatophores at 550 nm. The data are fitted to the sum of two exponentials with lifetimes of 0.27 and 1.8 ms and equal amplitudes. The difference between the experimental and fitted curves is shown below. Conditions: 20 mM Tris-HCl (pH 8.0)/100 mM NaCl/4 mM *o*-phenanthroline. 60 μM ferricyanide was also added to keep the E_h at about 450 mV in order to maintain the bound cytochromes oxidized.

The kinetics of $P^+Q_A^-$ charge recombination observed in chromatophores, in the presence of *o*-phenanthroline, display the same type of heterogeneity as in RCs. Fig. 3 shows the decay kinetics measured at 550 nm, at pH 8, at sufficiently high redox potential to oxidize all the bound cytochromes. The rates are somewhat higher than observed in RCs at the same pH (1.8 and 0.27 ms in chromatophores, 2.2 and 0.66 ms in RCs), and the amplitude ratio is 1, compared to 0.7(slow)/0.3(fast) in RCs. These data support the notion of an intrinsic heterogeneity of the recombination kinetics, rather than an artifactual one induced during the RC preparation.

Temperature-dependence of the recombination kinetics

The temperature-dependence of the recombination kinetics was studied at pH 9, in 60% glycerol and in aqueous solvent (Figs. 4 and 5). The slow and fast kinetic components were resolved either by a two-component exponential analysis at 450, 800 or 850 nm, or by isolating each component near the isosbestic point, as described above, at 832.5 nm for k_{slow} and 834 nm for k_{fast}.

The temperature-dependences of k_{slow} and k_{fast}, in 60% glycerol (Fig. 4), are similar to that reported previously for k_{total}, on the basis of which it was suggested that $P^+Q_A^-$ in *Rps. viridis* recombines by two competitive processes [13]. At temperatures above about 240 K, the recombination occurs predominantly via a thermally excited state, previously termed M, which appears to be P^+I^-. At low temperature, a plateau is reached and the limiting, temperature-independent value of k_{total} (k_T) represents the rate constant via a direct tunneling process. Since the electron transfer between $P^+Q_A^-$ and P^+I^- is rapid compared to the recombinative decay of P^+I^- [20], the observed recombination of $P^+Q_A^-$ was described by:

$$k_{total} = k_d \cdot \exp(-\Delta G/k_B T) + k_T \quad (1)$$

where k_d is the rate constant of charge recombination in M (P^+I^-), ΔG is the free energy difference between $P^+Q_A^-$ and P^+I^-, and k_B is Boltzmann's constant. The convolution of fast and slow phases in the overall kinetic gives rise to a shape for the temperature-dependence of k_{total} which, as noted previously [13], cannot be fitted to a single set of parameters in Eqn. 1. The dependences of k_{slow} and k_{fast} on temperature, that we observe here, can be described by two similar equations:

$$k_{slow} = k_d \cdot \exp(-\Delta G_{slow}/k_B T) + k_{Tslow}$$

$$k_{fast} = k_d \cdot \exp(-\Delta G_{fast}/k_B T) + k_{Tfast} \quad (2)$$

where ΔG_{slow} and ΔG_{fast} are the corresponding free energy differences for k_{slow} and k_{fast}, and k_{Tslow} and k_{Tfast} are the limiting values of k_{slow} and k_{fast} obtained at low temperature. k_d is taken to be the same in Eqns. 1 and 2, i.e., for all components. This implicitly assumes that any distinctions between the component phases do not arise from direct influences on the decay of P^+I^- to the ground state. This is not unreasonable for direct recombination to the ground state, which is expected to be very insensitive to small changes in the energy level of P^+I^- [16]. However, since k_d is a composite rate constant, including recombination via reexcitation to the excited singlet state as well as directly to the ground state, this may not be fully valid. Nevertheless, in *Rb. sphaeroides*, estimates of the relative contributions of these two pathways suggest that the former is a very minor path [21].

Although the general shape of the temperature-dependence is similar for all components, the transition between the thermally activated process and the activationless process is sharper in the slow than in the fast

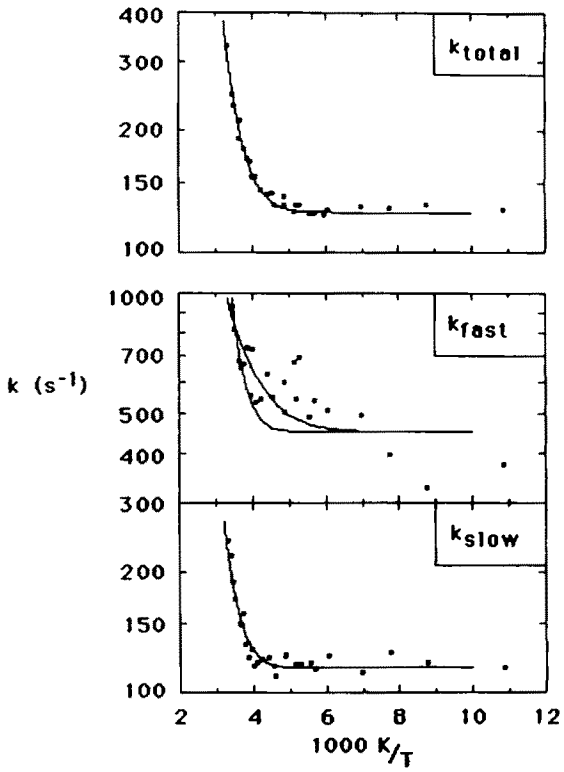

Fig. 4. Temperature-dependence of the rate constants for charge recombination in *Rps. viridis* RCs. Top: k_{total} determined from a one-component fit to the kinetic traces. Bottom: k_{fast} (upper set) and k_{slow} (lower set) determined from biexponential analysis of the data. Conditions: 60% glycerol/20 mM Tris-HCl (pH 9)/100 mM NaCl/4 mM *o*-phenanthroline. The lines are curves fitted according to Eqns. 1 and 2, in the form:

$$k = k_d \cdot \exp[\Delta S/k_B] \cdot \exp[-\Delta H/k_B T] + k_T$$

with $k_d = 2 \cdot 10^7\ s^{-1}$ for all curves. Other parameters were: for k_{total} $\Delta H = 0.226$ eV, $\Delta S = -0.24$ meV/K, $k_T = 125\ s^{-1}$; for k_{fast}, $\Delta H = 0.289$ eV, $\Delta S = 0.092$ meV/K (steeper curve) or $\Delta H = 0.123$ eV, $\Delta S = -0.5$ meV/K (flatter curve), $k_{Tfast} = 450\ s^{-1}$; for k_{slow}, $\Delta H = 0.273$ eV, $\Delta S = -0.13$ meV/K, $k_{Tslow} = 115\ s^{-1}$.

component. Also, in contrast with k_{total} and k_{slow}, k_{fast} seems to continue to decrease slowly below 250 K, possibly reaching a limiting value at about 120 K. However, the error in the measure of k_{fast} at low temperature is large because the relative amplitude of the fast phase, A_{fast}, decreases with temperature and is not more than 15% at temperatures below 250 K (Fig. 1).

The temperature-dependences of k_{total} and k_{slow} in glycerol (Fig. 4) were well fitted by Eqns. 1 and 2. k_{Tslow} and k_T were determined directly from the data to be $120 \pm 5\ s^{-1}$ and $128 \pm 4\ s^{-1}$, respectively. k_d was taken as $2 \cdot 10^7\ s^{-1}$, as discussed by Shopes and Wraight [13]. Fits to the data could be sensitively judged by visual inspection and, with a fixed value for k_d, required adjustments of both ΔH and ΔS. Best fits were obtained with $\Delta G_{slow} = 0.311$ eV and $\Delta G_{total} = 0.297$ eV. k_{fast} could not be reliably fitted because of the large uncertainty in the measured values below 250 K. Two very different fits, with the same ΔG value ($\Delta G_{fast} = 0.262$ eV), are shown to illustrate this point. The limiting value of k_{fast} is also somewhat uncertain, but a value of $420 \pm 50\ s^{-1}$ encompasses the likely range of possibilities. The derived data for all components are summarized in Table I.

TABLE I

Activation parameters for charge recombination in reaction centers from Rps. viridis

Component	k_T (s^{-1})	ΔH (eV)	ΔS (meV/K)	$-T\Delta S$ [a] (eV)	ΔG [a] (eV)
Total [b]	170	0.230	−0.172	0.051	0.281
	(±6)	(±0.004)	(±0.011)	(±0.003)	(±0.005)
Total [c]	128	0.226	−0.24	0.071	0.297
	(±4)	(±0.02)	(±0.07)	(±0.02)	(±0.02)
Fast [b]	460	0.278	0.058	−0.017	0.261
	(±60)	(±0.021)	(±0.065)	(±0.019)	(±0.022)
Fast [c]	420	– [d]	–	–	–
	(±50)	–	–	–	–
Slow [b]	155	0.258	−0.116	0.034	0.292
	(±10)	(±0.009)	(±0.034)	(±0.010)	(±0.011)
Slow [c]	119	0.273	−0.13	0.038	0.311
	(±6)	(±0.02)	(±0.07)	(±0.02)	(±0.02)

[a] $T = 298$ K.

[b] Temperature-dependence in aqueous buffer (pH 9). Data from Fig. 5: Arrhenius plots of $k - k_T$ vs. $1/T$, in the ambient temperature range, 280–320 K.

[c] Temperature-dependence in 60% glycerol (pH 9). Data from Fig. 4: fitted curves in the temperature range 90–310 K, using Eqn. 2.

[d] The extended temperature data for k_{fast} did not permit significant fits with Eqn. 2.

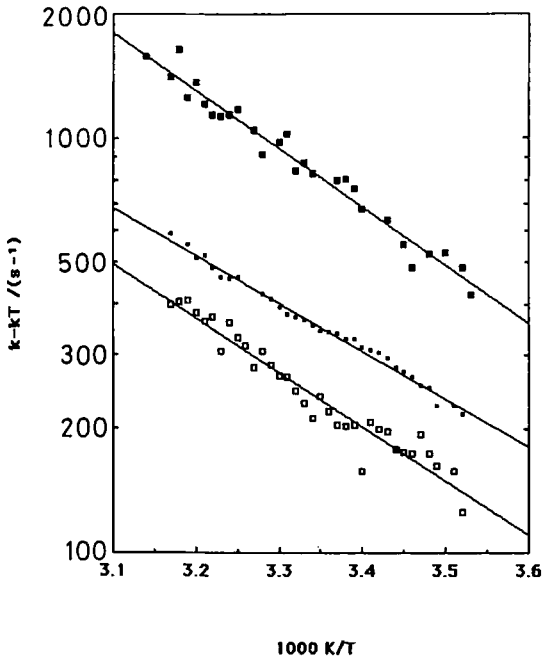

Fig. 5. Arrhenius plots of the rate constants of charge recombination in *Rps. viridis* RCs. The data are averages of sets obtained by two component analysis of the kinetics at 450, 800 or 850 nm, and by single-component fits to traces obtained at 832.5 nm (k_{slow}) or 834 nm (k_{fast}). All rates are plotted after subtraction of the limiting value obtained from low-temperature measurements in glycerol buffer and corrected as described in the text: $k_T = 170\ s^{-1}$, $k_{Tfast} = 460\ s^{-1}$ and $k_{Tslow} = 155\ s^{-1}$ (see text). Conditions: 20 mM Tris-HCl (pH 9)/100 mM NaCl/4 mM *o*-phenanthroline/0.1% LDAO. Symbols: k_{slow} (□), k_{fast} (■), k_{total} (●).

At 120 K, k_{slow} and k_{fast} were found to be pH-independent (within 10%) in the range pH 6–10.5 (not shown). This is consistent with the hypothesis that the low-temperature values of k_{slow} and k_{fast} are mainly governed by an activationless process that is essentially different from the thermal route.

Arrhenius analysis of the kinetics at ambient temperatures

The temperature-dependence of the recombination kinetics was measured over the range 280–320 K, using RCs in aqueous buffer (pH 9). In order to use an Arrhenius-type representation to obtain the activation parameters for the thermally excited decay route, it is necessary to subtract the appropriate temperature-independent rate constants from the net rate constants. However, we could not obtain values of k_{Tslow}, k_{Tfast} and k_T directly in aqueous buffer because of the light scattering of the frozen samples. Low-temperature values were obtainable in 60% glycerol, which, however, also slows down the kinetics [13]. To obtain the corresponding values in aqueous buffer we used the following procedure. k_{slow}, k_{fast} and k_{total} were measured at room temperature, in 0, 10 and 60% glycerol, and the ratio for each rate constant was calculated for 60/0% and 60/10% glycerol. The rate constants in 10 and 60% glycerol were then measured at low temperature. The ratio of rates for 60/10% glycerol was the same at low temperature as at room temperature and we assumed

that the ratio for 60/0% glycerol, measured at low temperature, was also unchanged compared to room temperature. We then applied this factor to the values of $k_{T\text{slow}}$, $k_{T\text{fast}}$ and k_T in 60% glycerol (see Fig. 4), to obtain the appropriate values in aqueous buffer. In aqueous buffer at pH 9, in the presence of *o*-phenanthroline, k_T, $k_{T\text{slow}}$ and $k_{T\text{fast}}$ were determined to be 170 ± 5, 155 ± 10 and 460 ± 60 s^{-1}, respectively. The corrections for k_T and $k_{T\text{slow}}$ were significant, with 60/10% ratios of 0.74 and 0.76, respectively, but 60% glycerol had a much smaller effect on $k_{T\text{fast}}$ with a correction factor of only 0.91. The value of k_T, obtained here, is significantly larger than that used by Shopes and Wraight who took the rate measured directly in 60% glycerol. However, the difference has very little effect (less than 5 meV) on the computed activation free energy, but is more influential on the relative contributions of ΔH and ΔS, as discussed in Ref. 13.

After correction for the low-temperature rates, the data are well-fit by straight lines in an Arrhenius plot (Fig. 5). The activation parameters of k_{slow}, k_{fast} and k_{total} are shown in Table I, and represent an average of three independent experiments. Two were obtained by a two-component decomposition of the kinetics at 450 and 800 nm. The third set was obtained near the isosbestic point, at 832.5 nm for k_{slow} and 834 nm for k_{fast}. There was good agreement between the two methods of kinetic analysis. The average ΔH values obtained from the slopes are 0.230 ± 0.003 eV for ΔH_{total}, 0.258 ± 0.009 eV for ΔH_{slow} and 0.278 ± 0.021 eV for ΔH_{fast}. The value for ΔH_{total} is significantly larger than that reported previously, for this pH (0.19 eV). This is entirely due to the different value used for k_T. As noted above, however, this has almost no effect on the activation free energy. From Eqn. 2, it can be shown that the intercepts of the Arrhenius plots with the ordinate give $\Delta S/k + \ln k_d$, for each component. Assuming a k_d value of $2 \cdot 10^7$ s^{-1} [13], one can calculate ΔS. As can be seen in Table I, the contributions of ΔS in ΔG are not negligible. ΔH_{fast} is greater than ΔH_{slow} or ΔH_{total}, whereas ΔG_{slow} (0.292 ± 0.011 eV) and ΔG_{total} (0.281 ± 0.004 eV) are greater than ΔG_{fast} (0.261 ± 0.022 eV) (Table I). At pH 9 and 298 K, the slow and fast components differ in ΔG by about 30 meV. This, of course, is consistent with the k_{slow} and k_{fast} values measured at pH 9. According to Eqn. 2, the ratio $(k_{\text{slow}} - k_{T\text{slow}})/(k_{\text{fast}} - k_{T\text{fast}})$, measured at pH 9, must match the term $\exp(\Delta\Delta G.kT)$, where $\Delta\Delta G = \Delta G_{\text{fast}} - \Delta G_{\text{slow}}$. This is the case within 10%.

The values for ΔG_{slow} and ΔG_{total} derived from the ambient temperature range were 17–20 meV smaller than those used to fit the extended temperature-dependences in Fig. 4. A similar discrepancy (8 meV) was noted earlier, comparing aqueous buffer and 60% glycerol, at pH 7 [13]. This deviation is within the error of the extended temperature-range measurements, but may also reflect a modulating effect of the glycerol in the ambient temperature range, perhaps through the viscosity-dependence noted earlier [13]. In view of this, the fact that the ratio of rates in 10/60% glycerol is the same at ambient and low temperatures indicates that the effect of glycerol and/or viscosity is not straightforward, and emphasizes the ad hoc nature of the correction we have applied to k_T. As for the rate constants, the effect of 60% glycerol, compared to aqueous solvent, seemed smaller on ΔG_{fast} than on ΔG_{slow} or ΔG_{total}.

pH-dependence of the rate constants and relative amplitudes of both components

The pH-dependence of the recombination kinetics was studied with or without *o*-phenanthroline. The overall kinetics (k_{total}) was determined as a single-exponential analysis of the decay at 450 nm. The two components, k_{slow} and k_{fast}, were obtained both by

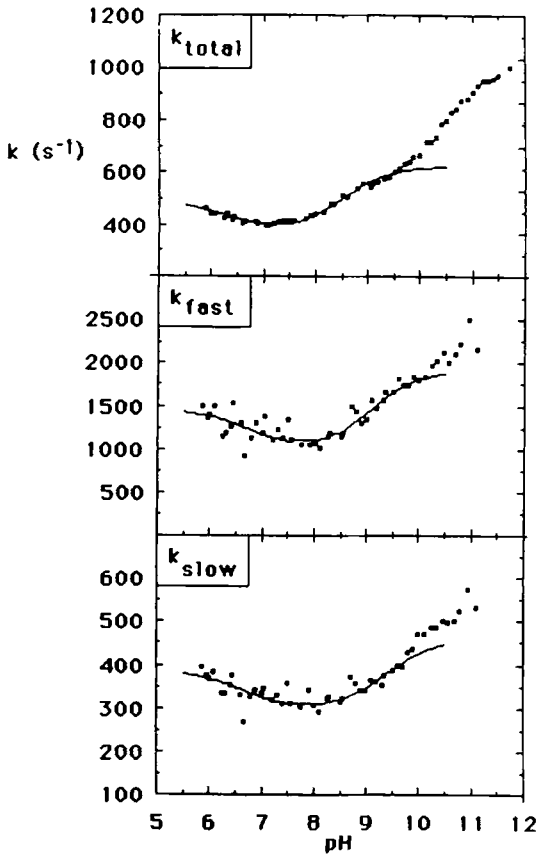

Fig. 6. pH-dependence of k_{total}, k_{fast} and k_{slow} in the presence of *o*-phenanthroline. Conditions: 100 mM NaCl/0.1% LDAO/4 mM *o*-phenanthroline. The lines are drawn according to Eqn. 5, considering two values for pK_{QA} for transitions between three protonation states of the RC. The recombination kinetics of each state are described by three different values of the free-energy difference between $P^+Q_A^-$ and P^+I^-, $\Delta G = \Delta G_{H^+} + \delta G$, where ΔG_{H^+} is the activation free energy at low pH (< pH 6) and δG is the free energy modulation caused by the different interactions between the protonation site and the negative charge of Q_A^- and I^-. Values for the fitting parameters, ΔG_{H^+}, pK and δG for each component, are summarized in Table II. k_d was taken equal to $2 \cdot 10^7$ s^{-1} for all fits.

decomposition of the kinetics at 450 nm and by measurements at 832.5 and 843 nm, where the slow and fast components, respectively, are almost pure. Both approaches gave similar data. All kinetic components – k_{total}, k_{slow} and k_{fast} – decreased slightly as the pH was raised from pH 5.7 to about 7.5, and then increased by a factor of 2–3 in the region pH 8–11.5, depending on the salt concentration (not shown) and on the presence of *o*-phenanthroline (Figs. 6 and 7).

The intrinsic nature of the heterogeneity in the recombination kinetics is well demonstrated by the pH-dependence of the relative amplitudes of the fast and slow components, in 10 mM NaCl (Fig. 8). These curves display two steps in the range of pH 6–12, and it seems clear that the two types of kinetic behavior are interconvertible in this pH range studied. There is no obvious correspondence between apparent pK values suggested by these curves and those associated with the pH dependences of k_{fast} and k_{slow} and the involvement of two pKs is not sufficient to understand the pH-dependence of rates and amplitudes of the recombination kinetics in *Rps. viridis* RCs. As discussed below, a minimum of three protonatable groups appears to be necessary to explain the pH-dependence of the rate constants, and the involvement of distinct pK values before and after the flash is evident in the pH-dependence of the compo-

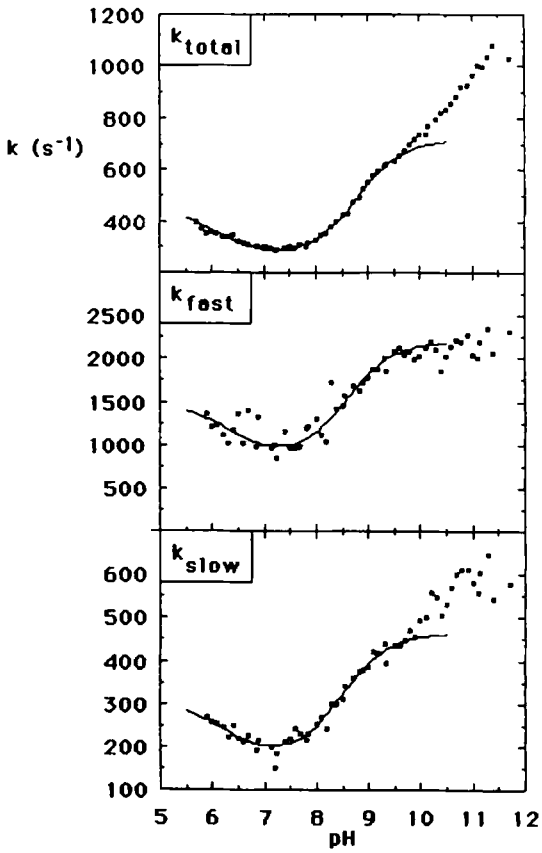

Fig. 7. pH-dependence of k_{total}, k_{fast} and k_{slow} in the absence of *o*-phenanthroline. Conditions as for Fig. 6, except without *o*-phenanthroline. The fitting parameters are summarized in Table II.

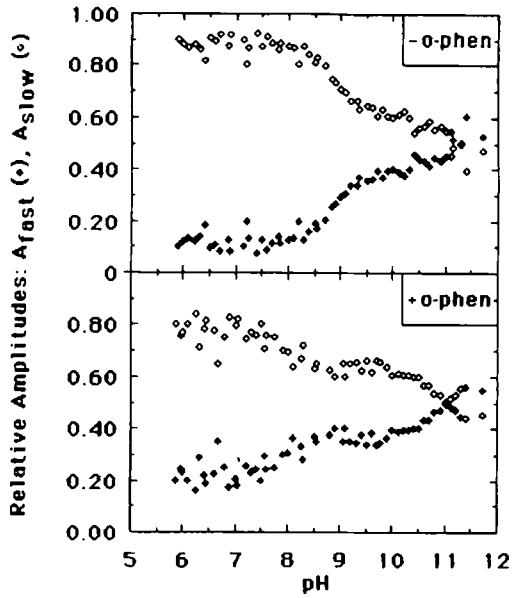

Fig. 8. pH-dependence of A_{slow} and A_{fast}, the relative amplitudes of the slow and fast kinetic phases of the charge recombination in *Rps. viridis* RCs. Conditions: 100 mM NaCl/0.1% LDAO, 20 °C. Top: without *o*-phenanthroline; Bottom: plus 4 mM *o*-phenanthroline. Open symbols; A_{slow}; closed symbols: A_{fast}.

nent amplitudes. It should be noted that the curves with and without *o*-phenanthroline are quite different, not only in terms of the pH at which the plateau is reached (approx. 8.6 with *o*-phenanthroline and approx. 9.5 without), but also because of the shape of the curve. The plateau is more clearly defined in the presence of *o*-phenenthroline, where A_{fast} stays roughly constant or even decreases from pH 9 to 10. These features were also markedly dependent on the concentrations of NaCl or $MgCl_2$, as will be presented elsewhere.

Discussion

In this study, we have demonstrated a previously unrecognized complexity of the charge-recombination kinetics in RCs from *Rps. viridis*. Since a similar biphasicity is observed in chromatophores and in isolated RCs, it is probable that the heterogeneity is intrinsic rather than artifactual in nature. Furthermore, the interconvertibility of the two phases with pH and with temperature implies the existence of two states within a single population of RCs, rather than two permanently distinct populations.

In *Rps. viridis*, at ambient temperatures, the $P^+Q_A^-$ state decays predominantly via P^+I^-, with which it is in thermal equilibrium [13]. The net recombination is described by Eqn. 1. Any change in ΔG between $P^+Q_A^-$ and P^+I^- due, for example, to differences in protonation behavior of the two states, will change the rate constant of charge recombination via the thermally activated route. Interaction between Q_A^- and a protonated site will lead to stabilization of the $P^+Q_A^-$ state,

thereby increasing ΔG and retarding the activated recombination process, while an interaction between I^- and a protonated site will stabilize P^+I^-, thereby decreasing ΔG and accelerating the activated recombination pathway. The net magnitude of ΔG will reflect the difference in the strengths of interaction between the protonation site and the two charged redox species, and the degree of protonation as determined by their effective pK values. If the protonation equilibria are established rapidly compared to the rate of recombination, the decay kinetics will be monophasic and the pH-dependence will be roughly sigmoidal, with turning points at pK_I and pK_{QA}, according to Ref. 13:

$$k_{obs} = k_d \cdot e^{-\Delta G_{H^+}/kT} \cdot \frac{1+10^{(pH-pK_I)}}{1+10^{(pH-pK_{QA})}} + k_T \qquad (3)$$

ΔG_{H^+} is the free-energy difference between $P^+Q_A^-$ and P^+I^-, at some arbitrary reference point in the low pH region. In an earlier report on the pH-dpendence of k_{total}, Shopes and Wraight used this description to propose that protonation in response to I^- and Q_A^- exhibited pK values of approx. 9.4 (pK_I) and approx. 9.7 (pK_{QA}) [13]. These values indicate a stronger interaction with Q_A^-.

Eqn. 3 can be written even more simply in terms of a modulation, by the H^+ ion, of the activation free energy, ΔG [22]. The pH-dependence is then described by a simple titration between two states in which the ΔG between $P^+Q_A^-$ and P^+I^- is modulated by an amount, δG, equivalent to the difference in pK values:

$$\delta G = 58 \cdot \delta pK \text{ meV} \qquad (4)$$

where δpK represents the difference, pK_I − pK_{QA}. A positive value implies that protonation stabilizes P^+I^- relative to $P^+Q_A^-$, leading to a more rapid charge recombination. The titration is characterized by a pK that is an average for the two charge-separation states, weighted by their relative abundance which greatly favors $P^+Q_A^-$, i.e., it is expected to be indistinguishable from pK_{QA}:

$$k_{obs} = k^{\ddagger} \cdot \frac{e^{\delta G/kT} + 10^{(pH-pK_{QA})}}{1+10^{(pH-pK_{QA})}} + k_T \qquad (5a)$$

where

$$k^{\ddagger} = k_d \cdot e^{-\Delta G_{H^+}/kT} \qquad (5b)$$

The pH-dependence of the rate constants, reported in this work, calls for an extension of this hypothesis, with more than one protonation site to account for the complexity of the curves. The trends in all components, k_{total}, k_{fast} and k_{slow}, are as reported previously for the overall kinetics [13], with a shallow minimum at pH 7–7.5 and substantial acceleration at high pH. The rate

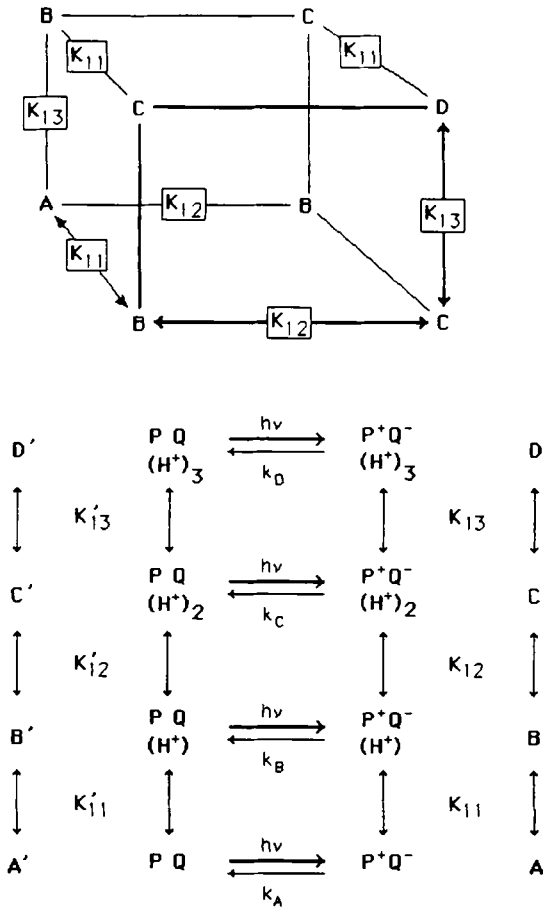

Fig. 9. Top: Generalized scheme for protonation states with three protonatable groups. A represents the fully deprotonated state, B denotes the three monoprotonated states, C the three diprotonated states and D is the fully protonated state. When all protonation sites are independent, there are only three distinct pK values, pK_{11}, pK_{12} and pK_{13}. If these pK values are not very close, net protonation can be described by the linear path shown by the three arrows. The apparent pK values for the three protonation steps are very similar to pK_{11}, pK_{12} and pK_{13}, unless the true pK values are almost equal. For n protonation sites, the maximum deviation between an observed pK and the corresponding true value is log n, i.e., 0.48 for $n = 3$, and occurs when pK_{11} = pK_{12} = pK_{13}. Bottom: Reduced (linear) scheme for independent protonation equilibria (three pK values), showing the correlation with the RC states. In general, distinct sets of equilibria ($K'_{11} - K'_{13}$ and $K_{11} - K_{13}$) apply to the dark-adapted and light-activated states of the RC, respectively.

enhancement seen as the pH is raised from 8 to 11.5 is not monotonic, however, suggesting the involvement of more than one titration step. An adequate description of the rate constant data might seem to be provided by a model with four protonation states, with distinct recombination rates covering the range from low to high. In its simplest form, this would involve three independent pK values, as shown in Fig. 9. The transition from each state to the next as the pH is raised would be accompanied by a change in the observed rate of recombination, as described by Eqn. 5.

However, at this point we note that the biphasicity of the recombination kinetics shows quite clearly that

complete equilibrium is not established at all pH values, and fails drastically above pH 10. Qualitatively, the complexity of the recombination kinetics depends on the relative rates of interconversion between the protonation states compared to the rate of recombination, which varies in the range 200–2000 s^{-1}. If the protonation states come into rapid equilibrium after the flash, the recombination kinetics will be monophasic with a pH-dependent, effective rate constant that is a weighted average of the four decay channels. For three independent protonation sites, this yields

$$k_{obs} = \frac{k_A[A] - k_B[B] + k_C[C] + k_D[D]}{[A]+[B]+[C]+[D]} + k_T \quad (6a)$$

$$= \frac{\{(k_A \cdot 10^{pH-pK_{11}} + k_B) \cdot 10^{pH-pK_{12}} + k_C\} \cdot 10^{pH-pK_{13}} + k_D}{(1+10^{pH-pK_{11}})(1+10^{pH-pK_{12}})(1+10^{pH-pK_{13}})} + k_T \quad (6b)$$

where k_i is the individual rate constant for recombination from each of the protonation states, i, and each rate constant can be defined by a value of δG or δpK. pK_{11}, pK_{12} and pK_{13} refer to the three independent protonation equilibria of Fig. 9 (pK_{QA} in Eqn. 5), with decreasing affinities.

If the protonation equilibria are not attained rapidly, then the mixture of protonation states undergoing recombination, after the flash, will be fixed in the distribution established in the dark, before the flash. In general, the dark pK values will be different from those in the light-activated state. Since each state may have inherently different recombination times, governed by δG as described above, the decay kinetics will be polyphasic. The observed decay phases will include not only the rate processes for recombination but also any rate-limiting values for the protonation and deprotonation steps. Taking a value of 10^{11} $M^{-1} \cdot s^{-1}$ for the bimolecular protonation rate constant, k_{H^+}, we find a net rate of protonation (k_{on}) in excess of 10^4 s^{-1} at pH values below 7. This is marginally sufficient to approach equilibrium on the time-scale of the slower recombination events. However, in extensive studies on proton uptake by RCs from *Rb. sphaeroides* we have observed the bimolecular rate constant for proton uptake to be significantly pH-dependent and much higher than 10^{11} $M^{-1} \cdot s^{-1}$ at high pH (greater than 10^{13} $M^{-1} \cdot s^{-1}$ above pH 11) (Maroti, P. and Wraight, C.A., unpublished observations). This arises from electrostatic effects on the local pH and on the rate processes near the protein surface [23]. With a value of 10^{12} $M^{-1} \cdot s^{-1}$ for k_{H^+}, quite rapid equilibration of the protonation states could be achieved at pH values up to 8. The data of Fig. 9 show that the recombination kinetics becomes more obviously biphasic at pH values above about 7.5 and 8 in the presence and absence of *o*-phenanthroline, respectively.

Numerical simulations based on the scheme of Fig. 9, indicated that the double wave of high and low amplitudes was generally attributable to two features, but the model is too heavily underdetermined to yield any unequivocal rate or equilibrium parameters. The increase in A_{fast} seen above pH 10.5 was found to be almost entirely a reflection of a dark pK value, i.e., in the PQ_A state, while the first increment in biphasicity at lower pH (onset at pH 7.5–8.5, plateau at pH 9–10) was largely due to convolution of kinetic processes after the flash. A model with three independent protonation sites has a relatively large number of microstates (eight), but the equilibria are dominated by four of these (see Fig. 9). Each of these must be assigned a different recombination rate constant to account for the pH-dependences observed, but the data only warranted analysis into two components. In view of the evidently incomplete equilibration of the protonation states, the slow and fast phases obtained cannot be eigenvalues of the canonical rate equation and may only be resultants of the forced biexponential analysis. Thus, as the pH is varied, the nature of the fast and slow phases may change, i.e., the components dominating the fast and slow phases at high pH are not the same as at low pH. However, at low pH, the kinetics are almost monophasic and the slow component presumably reflects a weighted average of the rate constants of the prevailing protonation states. This titrates quite smoothly from a value, in the absence of *o*-phenanthroline, of 400–500 s^{-1} at pH less than 6 to 200–300 s^{-1} at pH 7–7.5. The rates in the presence of *o*-phenanthroline are about 100 s^{-1} higher. At high pH, the kinetics are markedly biphasic. In view of the expected rates of protonation (i.e., $k_{on} = k_{H^+} \cdot 10^{-pH}$ approx. 1–10 s^{-1}, at pH 11) the two phases reflect the unaveraged characteristics of relatively deprotonated states in a population established according to the protonation equilibrium in the dark. The limiting values of k_{slow} and k_{fast}, at high pH, are 500–600 and 2000–2200 s^{-1}, respectively. The effect of *o*-phenanthroline is not marked in this region.

Below about pH 10, the kinetics, whether monophasic or not, are largely determined by events after the flash. In order to see, qualitatively, the trends in the recombination parameters over this pH range, we took the overall (one-component) analysis (k_{total}) as an approximation to the monophasic kinetic that would be observed if complete equilibration was established, and fitted it with an equation of the type shown by Eqn. 6b. Since the fit is truncated at pH 10, only two pK values are required (pK_{12} and pK_{13} in Fig. 9), describing three states (B, C and D) differing in their degree of modulation of the activation free energy (ΔG) for the thermal recombination route. The δG values can be determined from the rates observed at the end-points of each titration, after subtracting the low-temperature rate, k_T, which is not significantly affected by either the prevail-

TABLE II

pH-Dependence parameters for charge recombination in RCs from Rps. viridis

Component:	k_{total}			k_{fast}			k_{slow}		
	ΔG_{H^+} (eV)	pK_{Q_A}	δG (δpK) (meV)	ΔG_{H^+} (eV)	pK_{Q_A}	δG (δpK) (meV)	ΔG_{H^+} (eV)	pK_{Q_A}	δG (δpK) (meV)
+ *o*-Phen [a]	0.280	6.3	+11 (+0.19)	0.252	6.7	+13 (+0.24)	0.288	6.6	+12 (+0.20)
		8.5	−20 (−0.34)		9.1	−23 (−0.41)		9.4	−19 (−0.32)
− *o*-Phen [b]	0.284	6.1	+27 (+0.47)	0.251	6.3	+21 (+0.36)	0.299	6.2	+41 (+0.70)
		8.8	−44 (−0.76)		8.6	−34 (−0.58)		8.5	−58 (−1.0)

[a] Fitting parameters for curves in Fig. 6, in the range pH 6–10.
[b] Fitting parameters for curves in Fig. 7, in the range pH 6–10.

ing pH [13] or the presence of *o*-phenanthroline (not shown). In the absence of *o*-phenanthroline, the pH-dependence of k_{total} titrates in two waves, with pK values at pH 6.1 and pH 8.8, and δG (δpK) values of 27 (0.47) and −44 meV (−0.76), respectively. In the presence of *o*-phenanthroline, the pK values were similar (6.3 and 8.5) and the $\delta G(\delta pK)$ values were 11 (0.19) and −20 meV (−0.34), respectively (see Table II).

As expected from the general similarity of the pH-dependences of the various kinetic components, similar pK and δG (δpK) values were obtained by fitting the fast and slow components, separately. To fit the pH titration curves for k_{slow} and k_{fast}, k_T and ΔG_{H^+} were assigned in the range of values obtained from the low temperature (Fig. 4) and Arrhenius plots (Fig. 5), respectively. In the absence of *o*-phenanthroline, the values for ΔG_{H^+} were 5–10 meV higher than those used when *o*-phenanthroline was present. This is consistent with the higher ΔG observed previously for k_{total}, when *o*-phenanthroline was absent [13]. The results of all fits are summarized in Table II. The implication in all cases is of two protonation equilibria with opposite influences on δG: one with a pK of 6–6.5, where protonation effectively stabilizes P^+I^- relative to $P^+Q_A^-$, and one at about pH 9, where $P^+Q_A^-$ is relatively stabilized by protonation. These opposite effects can be rationalized in terms of the relative strengths of interaction of the two protonation sites with I^- and Q_A^-, as described above. In purely electrostatic terms, this means that the lower pK group is 'closer', in dielectric distance (εr), to I^-, while the high pK group is closer to Q_A^-.

Redox titrations of Q_A/Q_A^- in chromatophores have suggested that, in *Rps. viridis,* the pK of protonation of Q_A^- is about 7.6, in the absence of *o*-phenanthroline; in the presence of inhibitor, the pK is raised to 10 [24]. Similar data have not been reported for isolated RCs from this species, and experience with RCs from *Rb sphaeroides* does not encourage a simple correlation with the chromatophore data [25–27]. The pK values, deduced here from the recombination kinetics, do not reveal a direct equality with the known redox pK values in chromatophores.

It is of interest to note that studies on delayed fluorescence from chromatophores of *Rps. viridis* have suggested the existence of an ionizable group that stabilizes $P^+Q_A^-$ (relative to the excited singlet state, P*) with a pK near 8, in the presence of *o*-phenenthroline. This is comparable to the apparent pK of 8.5 indicated by the total (average) kinetic component of the charge recombination (Table II). Since the redox pK of Q_A/Q_A^- in chromatophores, in the presence of *o*-phenanthroline, is reportedly above pH 10, it would appear that the free energy level of $P^+Q_A^-$ is determined by more than one group. Recent experiments on the proton binding characteristics of RCs from *Rb. sphaeroides* have shown that the redox properties of Q_A/Q_A^- are, indeed, responsive to many ionizable groups [27]. The weak effect of *o*-phenanthroline, observed here on the recombination kinetics in isolated RCs of *Rps. viridis,* is not obviously consistent with the large effect it has on the E_m of Q_A/Q_A^- in chromatophores [24]. However, in *Rb. sphaeroides,* this effect of *o*-phenanthroline appears to derive from a reversal of the effect of quinol, which it displaces from the Q_B site [26]. On the other hand, effects of *o*-phenanthroline and related inhibitors on the protonation properties of the quinone complex are distinct and independent of Q_B [26,27]. Thus, in the absence of Q_B (i.e., excess quinone), as here, little effect of *o*-phenanthroline might be expected via an energetic role of the E_m of Q_A/Q_A^-. The small differences actually seen may reflect a direct effect of the inhibitor, perhaps via structural modifications of the RC propagated from the Q_B site where it binds.

Measurements at low temperatures have not revealed any marked dependence of the limiting low-temperature rates on pH in the range pH 6–10. Nevertheless, two phases are observed at low temperature, i.e., k_{Tslow} and k_{Tfast}, and the responsible states are apparently interconvertible as the amplitude of slow phase increases at lower temperatures and is by far the dominant phase below 250 K. Within the rather large error of the analysis of the low-temperature kinetics, the amplitudes of the two components do not exhibit a dependence on pH, but the available pH range (pH 6 to 10) may not be

sufficient to reveal it. Low-temperature measurements at pH values above 10 have proven difficult and unreliable and this is currently under further study. In any case, although the low-temperature, activationless recombination process might be expected to have some dependence on the overall free energy of the back-reaction (approx. 0.68 eV, above the pK of $Q_A^-/Q_A^-(H^+)$ [12,13]), the rate is unlikely to change much in response to the small modulations of the energy level of $P^+Q_A^-$ caused by protonation [16]. However, it may be sensitive to quite subtle structural changes. In this context, a very interesting result was reported by Kleinfeld et al. for RCs from *Rb. sphaeroides* [28]. Freezing during illumination trapped the RCs in a configuration that exhibited markedly different properties with respect to charge separation and recombination, compared to freezing in the dark. It was suggested that the binding of protons to the states $P^+Q_A^-$ or $P^+Q_B^-$, formed in the light, resulted in conformational changes that were retained after recombination at low temperature. Similarly, the acceleration of the back-reaction in *Rb. sphaeroides,* seen at low temperature (a factor of 2 to 4), has been suggested to arise from a change in the distance between P^+ and Q_A^- of only 0.1 nm [29].

Slight differences in the absorption spectra near the $P^+Q_A^-$ isosbestic point at 833 nm allowed us to discriminate between the slow and fast components. The spectral behavior is very similar to that observed by Parot et al. [30] in RC's of *Rb. sphaeroides* and *R. rubrum* at low temperature, near the isosbestic point at 801 nm. These authors also detected a heterogeneity of the charge recombination kinetics from $P^+Q_A^-$, which exhibited a bi-exponential decay, only at low temperature, with lifetimes of 36 and 11 ms. The amplitude ratio of these two components was 40 : 60, and was not sensitive to pH or any other physical parameter tested. This behavior is similar to the low-temperature behavior reported here for *Rps. viridis*; although we have not performed an extensive analysis of the amplitudes at low temperature, the overall kinetics were not sensitive to pH or to temperature below about 220 K.

The relationship between the low-temperature behavior, either in *Rps. viridis* or in *Rb. sphaeroides,* and the heterogeneous kinetics at ambient temperature reported here for *Rps. viridis* is obscure. Nevertheless, it seems that the observability of the biphasicity in *Rps. viridis* at ambient temperatures is dependent on the relative rates of protonation and charge recombination. We have investigated the general applicability of this suggestion to other species by considering that the failure to observe heterogeneous kinetics in *Rb. sphaeroides* arises from the inherently slow rate of charge recombination in that species ($\tau = 100$ ms). We have, therefore, replaced the native Q_A (ubiquinone-50 or Q_{10}) in RCs of *Rb. sphaeroides,* by quinones of low potential, such as anthraquinones, to produce fast kinetics of charge recombination ($t_{1/2}$ approx. 5 ms) similar to those observed in *Rps. viridis*. The results showed that, indeed, a similar kind of kinetic heterogeneity could now be seen at room temperature, varying with pH [31].

Acknowledgements

This work was supported by an NSF grant (DBM 86-17144) to CAW. P.S. gratefully acknowledges leave from CNRS, Gif-sur-Yvette, France.

References

1 Deisenhofer, J., Epp, O., Miki, K., Huber, R. and Michel, H. (1985) Nature (Lond.) 318, 618–624.
2 Michel, H., Epp, O. and Deisenhofer, J. (1986) EMBO J. 5, 2445–2451.
3 Allen, J.P., Feher, G., Yeates, T.O., Rees, D.C., Deisenhofer, J., Michel, H. and Huber, R. (1986) Proc. Natl. Acad. Sci. USA 83, 8589–8593.
4 Chang, C.H., Tiede, D., Tang, J., Smith, U., Norris, J. and Schiffer, M. (1986) FEBS Lett. 205, 82–86.
5 Allen, J.P., Feher, G., Yeates, Komiya, H. and Rees, D.C. (1987) Proc. Natl. Acad. Sci. USA 84, 5730–5734.
6 Allen, J.P., Feher, G., Yeates, Komiya, H. and Rees, D.C. (1987) Proc. Natl. Acad. Sci. USA 84, 6162–6166.
7 Williams, J.C., Steiner, L.A. and Feher, G. (1986) Proteins 1, 312–325.
8 Michel, H. and Deisenhofer, J. (1988) Biochemistry 27, 1–7.
9 Thornber, J.P., Cogdell, R.J., Seftor, R.E.B. and Webster, G.D. (1980) Biochim. Biophys. Acta 593, 60–76.
10 Woodbury, N.W. and Parson, W.W. (1984) Biochim. Biophys. Acta 767, 345–361.
11 Woodbury, N.W., Parson, W.W., Gunner, M.R., Prince, R.C. and Dutton, P.L. (1986) Biochim. Biophys. Acta 851, 6–22.
12 Carithers, R.P. and Parson, W.W. (1975) Biochim. Biophys. Acta 387, 194–211.
13 Shopes, R.J. and Wraight, C.A. (1987) Biochim. Biophys. Acta 893, 409–425.
14 Gunner, M.R., Liang, Y., Nagus, D.K., Hochstrasser, R.M. and Dutton, P.L. (1982) Biophys. J. 37, 226a.
15 Gopher, A., Blatt, Y., Schönfeld, M., Okamura, M.Y. and Feher, G. (1985) Biophys. J. 48, 311–320.
16 Gunner, M.R., Robertson, D.E. and Dutton, P.L. (1986) J. Phys. Chem. 90, 3183–3195.
17 Shopes, R.J. and Wraight, C.A. (1986) Biochim. Biophys. Acta 848, 364–371.
18 Okamura, M.Y., Isaacson, R.A. and Feher, G. (1975) Proc. Natl. Acad. Sci. USA 72, 3491–3495.
19 Stein, R.R. (1986) Ph.D. Thesis, University of Illinois at Urbana-Champaign.
20 Holten, D., Windsor, M.W., Parson, W.W. and Thornber, J.P. (1978) Biochim. Biphys. Acta 501, 112–126.
21 Budil, D.E. (1987) Ph.D. Thesis, University of Chicago.
22 Kleinfeld, D., Okamura, M.Y. and Feher, G. (1985) Biophys. J. 48, 849–852.
23 Klapper, I., Hagstrom, R., Fine, R., Sharp, K. and Honig, B. (1986) Proteins 1, 47–59.
24 Prince, R.C. and Dutton, P.L. (1978) in The Photosynthetic Bacteria (Clayton, R.K. and Sistrom, W.R., eds.), pp. 439–453, Plenum Press, New York.
25 Dutton, P.L., Leigh, J.S. and Wraight, C.A. (1973) FEBS Lett. 36, 169–173.

26 Wraight, C.A. (1981) Isr. J. Chem. 21, 348–354.
27 Maroti, P. and Wraight, C.A. (1988) Biochim. Biophys. Acta 934, 329–347.
28 Kleinfeld, D., Okamura, M.Y. and Feher, G. (1984) Biochemistry 23, 5780–5786.
29 Feher, G., Okamura, M.Y. and Kleinfeld, D. (1987) in Protein Structure: Molecular and Electronic Reactivity (Austin, R., Buhks, E., Chance, B., DeVault, D., Dutton, P.L., Frauenfelder, H. and Gol'danskii, V.I., eds.), pp. 399–421, Springer, New York.
30 Parot, P., Thiery, J. and Verméglio, A. (1987) Biochim. Biophys. Acta 893, 534–543.
31 Sebban, P. (1988) Biochim. Biophys. Acta 936, 124–132.